

Cytotoxic Effects of Combination of Oxidosqualene Cyclase Inhibitors with Atorvastatin in Human Cancer Cells

Davide Staedler,^{†,‡} Catherine Chapuis-Bernasconi,[†] Henrietta Dehmlow,[§] Holger Fischer,[§] Lucienne Juillerat-Jeanneret,^{*,†} and Johannes D. Aebi^{*,§}

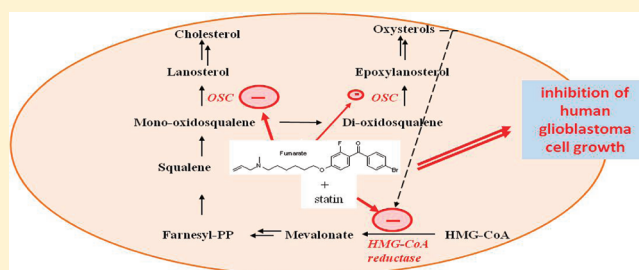
[†]Centre Hospitalier Universitaire Vaudois (CHUV) and University of Lausanne (UNIL), CH-1011 Lausanne, Switzerland

[‡]Institute of Chemical Sciences and Engineering, Ecole Polytechnique Fédérale de Lausanne, CH-1015, Lausanne, Switzerland

[§]F. Hoffmann-La Roche Ltd., Pharmaceutical Division, CH-4070 Basel, Switzerland

S Supporting Information

ABSTRACT: Ten oxidosqualene cyclase inhibitors with high efficacy as cholesterol-lowering agents and of different chemical structure classes were evaluated as potential anticancer agents against human cancer cells from various tissue origins and nontumoral human-brain-derived endothelial cells. Inhibition of cancer cell growth was demonstrated at micromolar concentrations, comparable to the concentrations of statins necessary for antitumor effect. Human glioblastoma cells were among the most sensitive cells. These compounds were also able to decrease the proliferation of angiogenic brain-derived endothelial cells, as a model of tumor-induced neovascularization. Additive effects in human glioblastoma cells were also demonstrated for oxidosqualene cyclase inhibitors in combination with atorvastatin while maintaining selectivity against endothelial cells. Thus, not only statins targeting the 3-hydroxy-3-methylglutaryl coenzyme A reductase but also inhibitors of oxidosqualene cyclase decrease tumor growth, suggesting new therapeutic opportunities of combined anti-cholesterol agents for dual treatment of glioblastoma.



■ INTRODUCTION

Cholesterol is an essential lipid in the body, in particular for the stability and function of cell membranes and cell organelles and for cellular trafficking.^{1,2} An excess of cholesterol causes lipid disorders, such as hypercholesterolemia.^{3,4} The rate-limiting enzyme for cholesterol biosynthesis is 3-hydroxy-3-methylglutaryl coenzyme A (HMG-CoA) reductase, and inhibitors of this enzyme, the statins, are used for the treatment of lipid disorders.^{3,4} In addition to their effects on hypercholesterolemia, statins were recently associated with a reduced risk of cancer progression, including melanoma, prostate, and colorectal cancers.^{5,6} These effects were in part due to the anti-inflammatory properties of statins, their inhibition of the mevalonate pathway, and HMG-CoA reductase-independent effects, such as the inhibition of protein–protein interaction.⁵

Inhibition of cholesterol synthesis by statins modifies the composition of the cell membrane via the reduction of the isoprenoids farnesyl pyrophosphate and geranylgeranyl pyrophosphate formation and the subsequent prenylation of small GTP-binding proteins. Statins also affect multiple cellular signaling pathways, such as the mitogen-activated protein kinases (MAPKs), phosphatidylinositol 3 kinase (PI3K), AKT (protein kinase B), and the epidermal growth factor receptor (EGFR).^{7,8} In vitro statins cause tumor-cell death and growth inhibition, and induce cell cycle arrest.^{9,10} In vivo, statins inhibit cancer growth, including neuroblastoma, glioma, acute

myeloblastic leukemia, and colorectal tumors.^{8,10} Statins have also shown antimetastatic activity^{11–14} and can act additively or synergistically with anticancer chemotherapeutic drugs.^{6,7,10} However, these effects were not always consistent, and it was suggested that the hydrophobicity of the statins is important for antitumor activity.¹⁵

Statin concentrations as anticancer agents is much higher than statin concentrations necessary as antihyperlipidemic agents. In the past years, novel synthetic inhibitors of HMG-CoA reductase activity that inhibit tumor cell proliferation and are structurally unrelated to existing statins have also been evaluated.¹⁶ Alternatively, new molecules that inhibit other enzymes of cholesterol biosynthesis, including inhibitors of the oxidosqualene/lanosterol cyclase (OSC) have been developed, also at Hoffmann-La Roche.^{16–23} However, until now these inhibitors have been evaluated only for their anti-cholesterol potential. In this work we evaluated whether inhibitors of OSC, like the statins, may also be potential anticancer agents, either alone or in combination with the statin atorvastatin.

OSC is an enzyme downstream of mevalonate synthesis involved in the biosynthesis of steroids and cholesterol. In cancer, the effects of statins are postulated to be related to the inhibition of the biosynthesis of mevalonate-derived farnesyl

Received: November 14, 2011

Published: April 26, 2012

and geranylgeranyl groups required for isoprenylation of oncogenic proteins. Mevalonate is the initial molecule of diverse pathways important for signaling in cell growth, proliferation, migration, and survival. The inhibition of HMG-CoA reductase by statins results in a few hours in an increased level of the protein as a net result of a feedback mechanism, thus reducing the efficacy of the statins. The enzymatic-mediated biosynthesis of steroids, downstream of HMG-CoA reductase, originates with farnesyl pyrophosphate through reductive dimerization to squalene, then conversion of squalene to lanosterol through epoxidation of squalene by squalene epoxidase to produce 2,3-oxidosqualene. OSC then generates the tetracyclic precursor of cholesterol, lanosterol. Synthesis of 24(S),25-epoxycholesterol is favored over cholesterol synthesis under conditions of partial OSC inhibition, whereas complete OSC inhibition results in decreased synthesis of cholesterol and 24(S),25-epoxycholesterol. Because 24(S),25-epoxycholesterol not only represses HMG-CoA reductase activity but also enhances its degradation, this should result in the generation of a synergistic, self-limited, negative regulatory feedback loop.^{17,24–28} Therefore, the first aim of our work was to evaluate new OSC inhibitors (OSCi) as *in vitro* anticancer agents, either as single agents or in combination with the statin atorvastatin, against human cancer cells of diverse origins, then to focus on human glioblastoma cells and human angiogenic brain-derived endothelial cells, hypothesizing that mevalonate depletion in tumor cells or endothelial cells may contribute to inhibition of tumor growth and angiogenesis.

CHEMISTRY

The syntheses and characterization of compounds **1**, **2**, **3**, **4**, **8**, and **9**^{17–20,29} have been previously described (structures shown in Table 1). Here we describe the syntheses of the alkyne-cyclohexyl inhibitors (compounds **5** and **6**, Scheme 1) and of the cyclohexylethyl inhibitor (compound **7**, Scheme 2) in which the cyclohexyl moiety of the already known compound **8**²⁹ was moved closer to the amine. Then the replacement of this important amine by an amide (compound **10**, Scheme 3) was done with only a minimal loss of inhibitory activity. Compound **1**,²⁰ bearing a rigid triphenyl ketone system, mimics the high energy intermediate of oxidosqualene cyclization to lanosterol.^{30,31} The benzylamine moiety of **1** was replaced by an oxyalkylamine (compound **2**),¹⁷ and the benzophenone was replaced by a heteroaryl (compounds **3** and **4**),^{19,29} by an alkyne cyclohexylcarbamate (compounds **5** and **6**), or an alkyne-cyclohexyl system (compounds **8** and **9**).²⁹

The synthesis of the alkyne OSCi is depicted in Scheme 1. Starting from *trans*-aminocyclohexanecarboxylic acid **11**, the aldehyde **12** was synthesized via the formation of the Weinreb amide, N-methylation of the Boc-protected amine, and lithium aluminum hydride reduction of the Weinreb amide. Corey–Fuchs alkyne introduction³² was followed by reaction with the appropriate halogenide to give intermediate **14**. Selective O-deprotection, mesylation, and cleavage of the Boc-protecting group using TFA gave amine **15**, which was converted to carbamate **16**. Amination and salt formation gave the two alkynes **5** and **6**. The synthesis of cyclohexylethyl linked OSCi **7** is described in Scheme 2. Silyl protected *trans*-cyclohexyl **17**³³ was hydrogenated and deprotected with platinum oxide in ethanol/chloroform to form hydrochloride **18**, which after Boc protection and N-methylation gave alcohol **19**. Mesylation and deprotection provided amine **20** as the hydrochloride which could be reacted with the *in situ* generated N-methylated

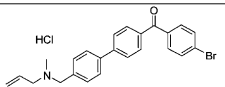
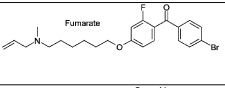
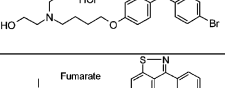
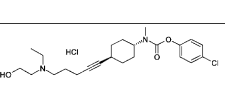
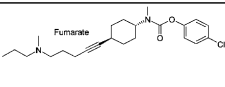
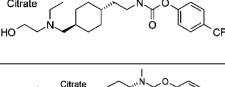
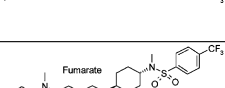
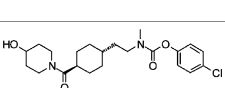
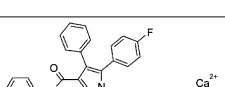
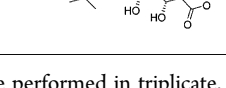
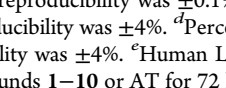
imidazole-1-carboxylic acid 4-trifluoromethylphenyl ester to give carbamate **21**. After reaction of **21** with ethyl-(2-hydroxyethyl)amine, compound **7** was converted to its citric acid salt and isolated by crystallization. The preparation of amide **10** is shown in Scheme 3. Building block **19** was oxidized to carboxylic acid **22** using Sharpless conditions,³⁴ and *N*-Boc deprotection yielded amino acid **23** as the hydrochloride salt. After heating in hexamethyldisilazane, the persilylated amino acid was reacted with 4-chlorophenyl chloroformate. Hydrolysis of the silyl ester during workup and coupling with 4-hydroxypiperidine gave amide **10**.

RESULTS AND DISCUSSION

All compounds selected for the present experiments demonstrated the highest efficacy out of their congeners in the respective chemical class as cholesterol lowering agents in the hamster model of hypercholesterolemia (results not shown). The most advanced OSCi, compound **5**, had been previously shown to decrease very low density lipoproteins (VLDL) and low density lipoproteins (LDL) apoB100 in miniature pigs.²² For *in vivo* evaluations and the present experiments, the metabolic stability of the OSCi was determined in rat hepatocytes, assessing the efficacy and potency of each compound in reducing cholesterol production while increasing monooxidosqualene (MOS) levels.¹⁹ The newly synthesized carbamates **5**, **6**, and **7** showed residual inhibitory activities greater than or equal to 60% after 24 h at 300 nM (Supporting Information Table S2). Amide **10**, which was structurally the least related OSCi, was less stable (76% inhibition after 8 h and 8% inhibition after 24 h). We also investigated the chemical stability at pH 4 and 7.4 at 37 °C and found no degradation of the OSCi. However, we observed lower recovery rates for compounds **2**, **4**, **6**, and **8** at pH 7.4, which is probably due to difficulties in keeping the compound in solution at this pH. However no degradation products were identified (Supporting Information Table S2).

First we evaluated the OSCi in human cells, 11 cancer cell lines from various tissue origins, and 1 nontumoral human brain-derived endothelial cell line (HCEC). Only compounds **1**, **2**, **3**, **4**, and **8** displayed efficient antiproliferative properties toward the majority of the cell lines after 24, 48 or 72 h of exposure (Supporting Information Table S3). The efficacy increased with the time of exposure, starting already after 24 h of exposure. In human cancer cells, the IC₅₀ values were dependent on the particular cell line considered (Table 2 and Figures 1 and 2). In human brain-derived LN18 and LN229 glioblastoma cells and HCEC brain-derived endothelial cells compounds **1**, **2**, **3**, and **4** were the most efficient compounds, displaying IC₅₀ values lower than 10 μM for at least one tumor cell line (Table 2 and Figures 1 and 2), compound **1** being the most selective compound for tumor cells compared to nontumoral HCEC cells. Atorvastatin (AT) also displayed some selectivity for human brain-derived tumor cells compared to endothelial cells but became active only after 72 h of cell exposure. The effect of OSCi or AT on DNA synthesis by these cells exposed to the compounds for 24 h was also determined using the thymidine incorporation assay. As for cell survival assays, OSCi compounds **2**, **3**, and **4** were the most active inhibitors of DNA synthesis of the series against the three cells (Figure 3 and Supporting Information Table S4). OSCi compounds **1** and **5–9** decreased DNA synthesis with less efficacy than OSCi compounds **2**, **3**, and **4**, but the effects were comparable in the three cells, whereas AT and OSCi **10** were less

Table 1. Structure and in Vitro Properties of the OSCi and AT

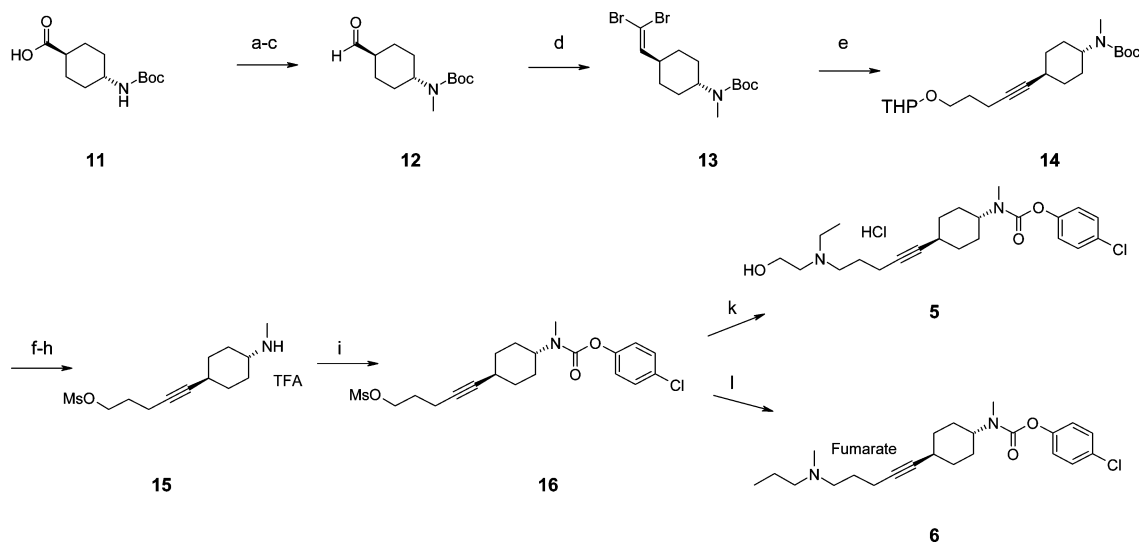
Cpd	Structure	Inhib. Hum. OSC ^a IC ₅₀ [nM]	logD ^b (pH 7.4)	PAMPA ^c P _e [x10 ⁻⁶ cm/s] pH 6.5	PAMPA ^d Membrane [%] pH 6.5	LN18 ^e IC ₅₀ [μM]	LN229 ^e IC ₅₀ [μM]	HCEC ^e IC ₅₀ [μM]
1		8.0	3.13	0.64	58	2.3	17.9	>30
2		5.7	3.92	0.12	20	6.1	8.8	3.8
3		17.8	3.39	0.22	37	2.0	2.9	2.2
4		2.9	3.43	0.57	40	7.6	5.2	4.8
5		10.0	2.51	2.87	10	13.4	21.1	29.1
6		7.8	3.28	0.81	0	28.0	>30	26.3
7		12.7	2.53	5.11	5	18.9	>30	>30
8		5.0	3.48	13	25	2.8	8.3	5.1
9		11.2	3.07	1.79	50	>30	>30	19.0
10		28.7	2.93	5.05	2	>30	>30	>30
AT		na	0.98	5.01	20	6.9	8.1	20.3

^aAll potency measurements were performed in triplicate. The standard error of the mean (sem) ranged between 10% and 20%. ^bAll measurements were done in triplicate, and the reproducibility was $\pm 0.1\%$. ^cApparent permeability P_e from the PAMPA assay at pH 6.5;³⁵ All measurements were done in triplicate, and the reproducibility was $\pm 4\%$. ^dPercent of the compound binding to the PAMPA lipid membrane; all measurements were done in triplicate, and the reproducibility was $\pm 4\%$. ^eHuman LN229, LN18, and HCEC cells were exposed to increasing concentrations (0, 2, 5, 10, 20, and 30 μM) of the OSCi compounds 1–10 or AT for 72 h. Then the MTT assay was performed and the IC₅₀ values were calculated. Results are the mean (standard deviations not shown, $\leq 10\%$) of triplicates of two independent experiments.

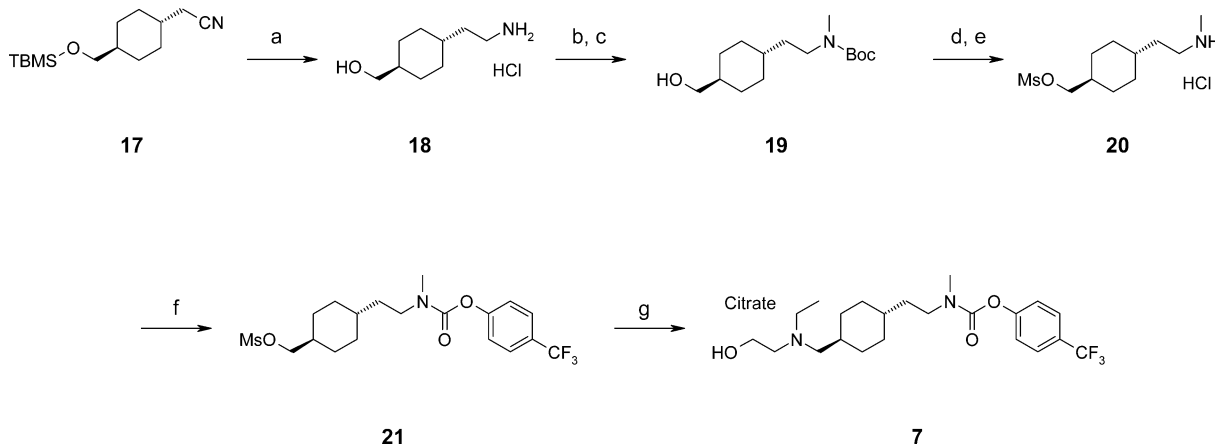
efficient in inhibiting DNA synthesis in endothelial cells compared to glioblastoma cells (Figure 3 and Supporting Information Table S4). These results suggest an initial cytostatic effect of both OSCi and AT in human glioblastoma cells.

Thus, for further experiments, combining an OSCi with AT, we selected the most active OSCi compounds 1, 2, 3, and 4 and the LN18 and LN229 cells as models of human glioblastoma cells and the nontumoral HCEC endothelial cells as model of nontumoral angiogenic brain-derived endothelial cells. Compounds 1, 2, 3, and 4 at three different concentrations (2, 4, and 10 μM) were combined with three different concentrations of AT (2.5, 5, and 10 μM) for 72 h because for this treatment time, AT as single agent dose-dependently reduced cell survival more in LN18 and LN229 glioblastoma cancer cells than in nontumoral HCEC cells.

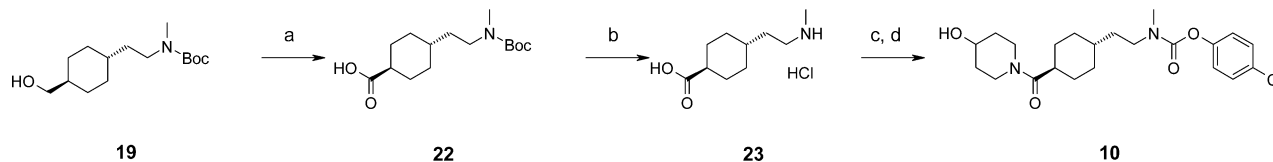
Compound 1 with AT combinations did not enhance the cytotoxic effects of each drug separately (data not shown). In LN18 cells exposed to compound 2, a cytotoxicity-enhancing effect of AT was seen at 2 and 4 μM compound 2. In LN229 cells exposed to 2 μM compound 2, a cytotoxicity-enhancing effect was detected well below the IC₅₀ values of both inhibitors. In HCEC cells, only at the highest concentrations of the OSCi (4 and 10 μM) was the AT effect on cell death seen (Figure 4). In LN18 cells exposed to compound 3, the addition of AT only decreased the survival of cells after exceeding the IC₅₀ of AT. In LN229 cells exposed to 2 μM compound 3, the addition of 2.5 μM AT decreased cell survival by 80%. With higher concentration of compound 3 in LN18 and in LN229 cells, only the cytotoxic effect of the increased concentrations of the OSCi was seen. In HCEC cells no

Scheme 1. Synthesis of the Alkyne OSCi Compounds 5 and 6^a

^aReagents and conditions: (a) MeOMeNH·HCl, HOBT, NMM, EDCl, CH₂Cl₂, 0 °C to rt, quantitative; (b) NaH (55% in oil), MeI, DMF, 0 °C to rt, 84%; (c) LAH, THF, 0–15 °C, quantitative; (d) Ph₃P, CBr₄, Et₃N, CH₂Cl₂, 0 °C to rt, 62%; (e) (1) *n*-BuLi, THF, –78 °C; (2) DMPU; (3) 2-(2-bromoethoxy)tetrahydro-2H-pyran, THF, –78 °C to rt, 40%; (f) PPTs, MeOH, 55 °C, 77%; (g) MeSO₂Cl, pyridine, DMAP, CH₂Cl₂, 0 °C to rt, quantitative; (h) TFA, CH₂Cl₂, 0 °C, quantitative; (i) 4-ClPhOCOCl, *i*-Pr₂NEt, CH₂Cl₂, 0 °C to rt, quantitative; (k) (1) ethyl-(2-hydroxyethyl)amine, MeOH, 65 °C; (2) HCl in dioxane, 59%; (l) (1) *N*-methylpropylamine, NaI, MeOH, 60 °C; (2) fumaric acid, EtOAc, EtOH, 76%.

Scheme 2. Synthesis of the Methylethylcyclohexyl OSCi 7^a

^aReagents and conditions: (a) PtO₂, H₂ (1 atm), EtOH/9% CHCl₃, 97%; (b) (1) (Boc)₂O, Et₃N, CH₂Cl₂, rt; (2) Ac₂O, pyridine, CH₂Cl₂, rt; (3) MeI, NaH (55% in oil), DMF, 0 °C to rt, 68%, three steps; (c) K₂CO₃, MeOH, rt, 86%; (d) MeSO₂Cl, Et₃N, CH₂Cl₂, 0 °C to rt, quantitative; (e) 4 M HCl in dioxane, rt, 92%; (f) (1) 4-trifluoromethylphenol, 1,1'-carbonyldiimidazol, CH₂Cl₂, rt; (2) (CH₃)₂SO₄, Hünig's base, CH₃CN, 80 °C; (3) 20, Hünig's base, CH₃CN, rt, 89%; (g) (1) ethyl-(2-hydroxyethyl)amine, DMA, 60 °C; (2) citric acid monohydrate, EtOAc, *i*-PrOH, *n*-pentane, 62%.

Scheme 3. Synthesis of the Amide OSCi 10^a

^aReagents and conditions: (a) NaIO₄, RuCl₃·H₂O, CH₃CN, CCl₄, H₂O, rt, 96%; (b) 4 M HCl in dioxane, rt, quantitative; (c) (1) HMDS, 145 °C; (2) 4-ClPhOCOCl, *i*-Pr₂EtN, THF, 0 °C to rt, 57%; (d) (1) (COCl)₂/DMF, CH₂Cl₂, 0 °C to rt; (2) 4-hydroxypiperidine, CH₂Cl₂, 97%.

cytotoxicity-enhancing effect of compound 3 with AT was observed (Figure 5). In LN18 cells exposed to compound 4 a cytotoxicity-enhancing effect with AT was seen. In LN229 cells

exposed to 4 μM compound 4, a pronounced cytotoxicity-enhancing effect with AT was demonstrated. In HCEC cells only the OSCi inhibitory effect was apparent (Figure 6).

Table 2. IC₅₀ after 72 h of Cell Exposure to Compounds 1–10 and AT^a

	IC ₅₀ (μM)								
	A549	CaCo2	HeLe	KB	LnCap	LNZ308	MCF-7	Me300	OVCAR
1	6.19	3.81	2.69	2.03	5.07	14.4	25.7	13.9	>30
2	11.3	2.99	2.89	2.88	>30	5.26	6.77	>30	>30
3	5.14	1.04	6.37	4.66	>30	4.7	5.58	6.2	16.7
4	6.06	1.97	8.85	8.52	19.5	4.4	8.3	13.4	>30
5	13.59	4.81	8.64	5.86	23.6	15.3	>30	26.2	>30
6	8.41	6.75	6.82	4.53	18.7	12.6	>30	18.9	>30
7	22.7	10.0	10.0	10.0	>30	23.2	>30	>30	>30
8	6.93	6.3	1.06	1.02	4.62	2.1	20.7	16.0	12.94
9	6.09	2.67	4.53	4.28	>30	>30	12.3	20.9	>30
10	>30	>30	21.8	7.58	5.55	>30	>30	25.0	>30
AT	>30	18.7	4.22	1.97	>30	7.44	>30	1.2	>30

^aCells were treated with increasing concentrations (0, 2, 5, 10, 20, and 30 μM) of the OSCi compounds 1–10 and AT for 72 h. Then the MTT assay was performed and the IC₅₀ values were calculated. Results are the mean (sd not shown, ≤10% of the mean) of triplicates of two independent experiments. IC₅₀ values for LN18, LN229, and HCEC cells are provided in Table 1 and Figures 1 and 2.

Acetate is a precursor in the biosynthesis of cellular lipids, including sterols, lipoproteins, and glycolipids; thus, we evaluated the incorporation of radioactive acetate in trichloroacetic acid (TCA) precipitable high molecular weight cellular molecules and/or acid insoluble lipids in glioblastoma cells exposed to increasing concentrations of AT and OSCi 2 or 3 (Figure 7). AT dose-dependently decreased ¹⁴C-acetate incorporation in the LN229 cells and to a lesser extent in LN18 cells. Both OSCi compounds 2 and 3 increased the ¹⁴C-acetate incorporation in both cell lines. From the known different mode of action of these molecules, this result was not unexpected and we can propose the following hypothesis. Statins inhibit at an early step of the biosynthesis of sterols, preventing accumulation of insoluble radioactive intermediates, while OSC inhibition would result in the accumulation of insoluble 2,3-oxidosqualene²⁵ and/or additional high molecular weight molecules, such as lipoproteins. In the glioblastoma cells, the increase in the incorporation of ¹⁴C-acetate induced by OSCi 2 was inhibited by AT addition, while for compound 3 the addition of AT had only a marginal influence (Figure 7). Thus, also in human glioblastoma cells different cellular pathways can be selectively inhibited by an OSCi and a statin, as previously shown for other human cancer cells.³⁵

Then the evaluation of possible additivity or synergism of OSCi and AT combinations was examined for combinations statistically significant using first for screening purposes the median effect model proposed by Chou.³⁶ This method proposes that a calculated combination index (CI) of ~1 defines additivity and that CI < 1 defines synergism. First, the CI factor was calculated to select combinations with possible additive or synergistic effects (Supporting Information Table S5). An additive effect was shown for a combination of AT with low concentrations of OSCi compounds 2, 3, and 4 in LN18 cells and OSCi compounds 2 and 3 in LN229 cells but only with high concentrations of OSCi 2 in HCEC cells (Supporting Information Table S5). Combination of AT with low concentration of OSCi 3 in LN229 cells provided CI < 0.5. Thus, for this combination, the computational method proposed by Lee et al.³⁷ was used to determine a possible synergism. According to this model, the interaction index (II) should be < 1 and its confidence interval should not include 1 to prove synergism; otherwise, the combined effect is additive. For the combination of 3 with AT in LN229 human glioblastoma cells, the confidence interval included 1 (Supporting Information Figure S1); thus, this combination did

not suggest a possible synergism. Therefore, the additive effect of OSCi with AT in LN18 cells and LN229 cells does not appear to be dependent on the chemical structure class of the compounds, since these effects were observed for two different classes of OSCi but may depend on the physicochemical and/or biochemical characteristics, i.e., membrane permeability and hydrophobicity, which were determined (Table 1) according to published procedures.^{38,39} From this information, it can be ruled out that limited cell membrane permeability was responsible for the observed effect, since the PAMPA (parallel artificial membrane permeation assay) membrane permeability (P_e PAMPA) was medium to high for all compounds (Table 1). The only correlation we found was the correlation between the ratios of their cytotoxicity potency for the human brain-derived endothelial cells to the two human glioblastoma cells ($IC_{50}(HCEC)/IC_{50}(LN229)$ or $IC_{50}(HCEC)/IC_{50}(LN18)$) (Figure 8). For only log *D* at pH 7.4 an inverse correlation between the IC₅₀ ratios of HCEC to LN18 and LN229 cells (Figure 8) was observed. However, the log *D* of AT (0.98) exerted a large influence on the plot. Thus, more polar OSCi compounds are more selective for inhibiting LN229 or LN18 growth, compared to nontumoral HCEC cells. It is interesting to note that the membrane fraction (Table 1) measured in the PAMPA experiment did not correlate with the selectivity ratio ($IC_{50}(HCEC)/IC_{50}(LN229)$, $r^2 = 0.05$) or the selectivity ratio ($IC_{50}(HCEC)/IC_{50}(LN18)$, $r^2 = 0.09$). Hence, it can be excluded that the difference in unspecific binding to either of the cell membranes governs the observed selectivity. This suggests that log *D* (pH 7.4) must be taken into account for further development of selective anticancer therapeutic compounds.

CONCLUSION

We have evaluated several chemical classes of our best inhibitors of OSC, an enzyme downstream of the HMG-CoA reductase in the mevalonate pathway. We show here that OSCi compounds have the potential to decrease the growth of human cancer cells of diverse tissue origin at micromolar concentrations, comparable to the concentrations of statins necessary for antitumor effect. Human glioblastoma and brain-derived endothelial cells, as a model of tumor-induced angiogenic endothelial cells, were among the most sensitive cells. It has been shown that the brain is the most cholesterol-rich organ of the body and the intensive cholesterol metabolism in brain tumors cells, higher than in nontumoral cells,^{40–44} suggests that the

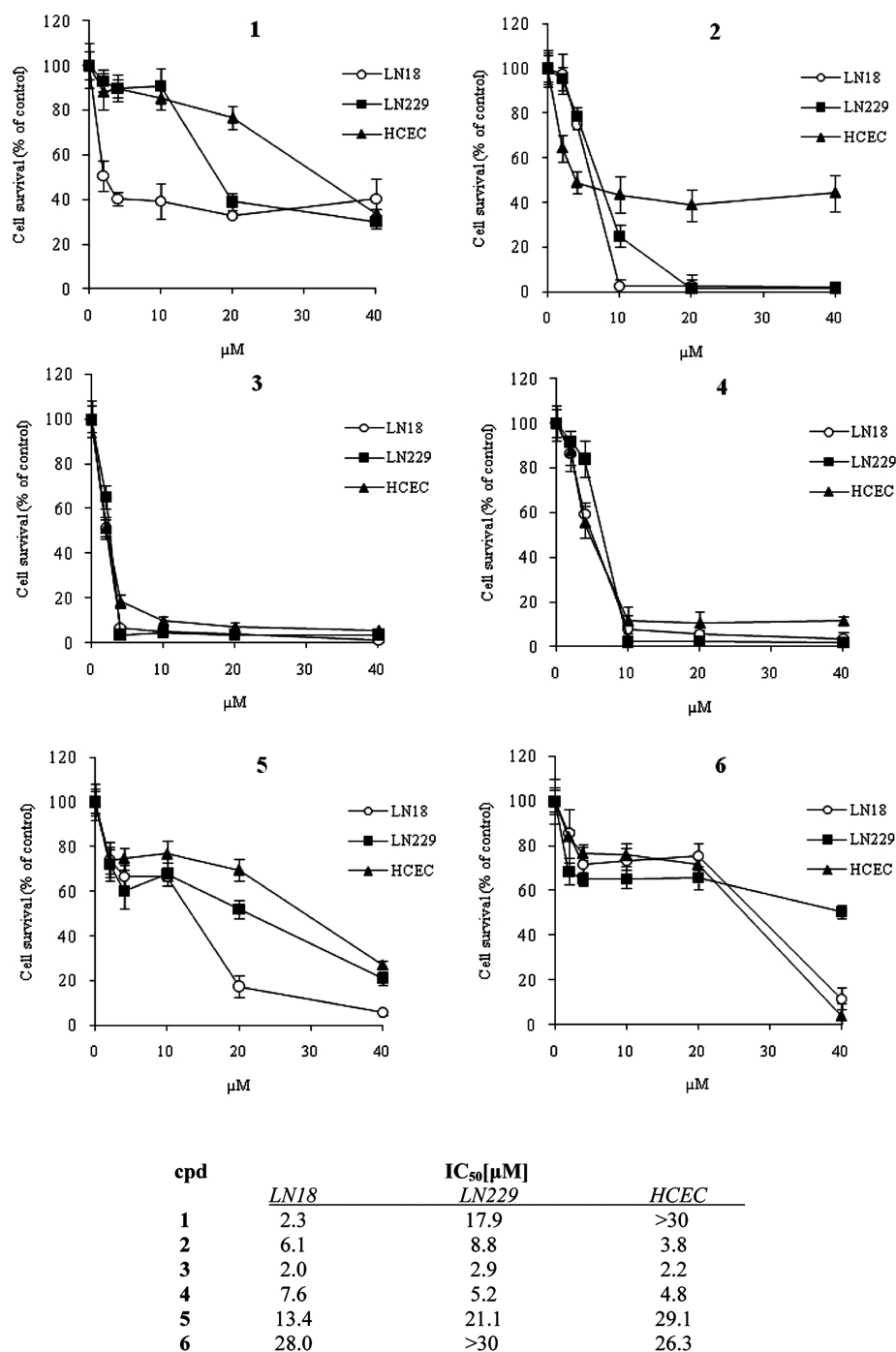


Figure 1. Cytotoxic effects of a 72 h exposure of human glioblastoma and brain-derived endothelial cells to OSCi compounds 1–6. Human LN18, LN229, and HCEC cells were exposed to increasing concentrations of compounds 1–6 for 72 h. Then the MTT assay was performed and IC₅₀ values were calculated. Results are the mean \pm sd of triplicates of two independent experiments. IC₅₀ values are the mean (sd not shown, $\leq 10\%$ of the values of the means) of triplicates of two independent experiments.

cholesterol pathway is a possible target for a specific pharmacological treatment of these tumors, thus opening interesting perspectives for the treatment of these very aggressive brain tumors. Previous studies have suggested that statins may have some antitumoral effect in brain cancers.^{45–50} A phase I–II trial of lovastatin for anaplastic astrocytoma and glioblastoma multiforme showed that high doses of lovastatin did not induce toxicity to the central nervous system (CNS).⁵¹ However, the concentrations of statins necessary to achieve anticancer effects were shown to be 10–100 times higher than their

concentrations as cholesterol-lowering drugs, suggesting that drug combinations must be developed. We found that not only statins, targeting the HMG-CoA reductase, but also inhibitors of the OSC decrease tumor cell growth and that their combination enhances their antitumoral efficacy. As statins are known to up-regulate HMG-CoA reductase expression and as 24(S),25-epoxycholesterol, a product of the OSC, decreases HMG-CoA reductase activity and enhances its degradation, OSC was postulated to be an interesting target in combination with a statin, since this should result in the generation of a

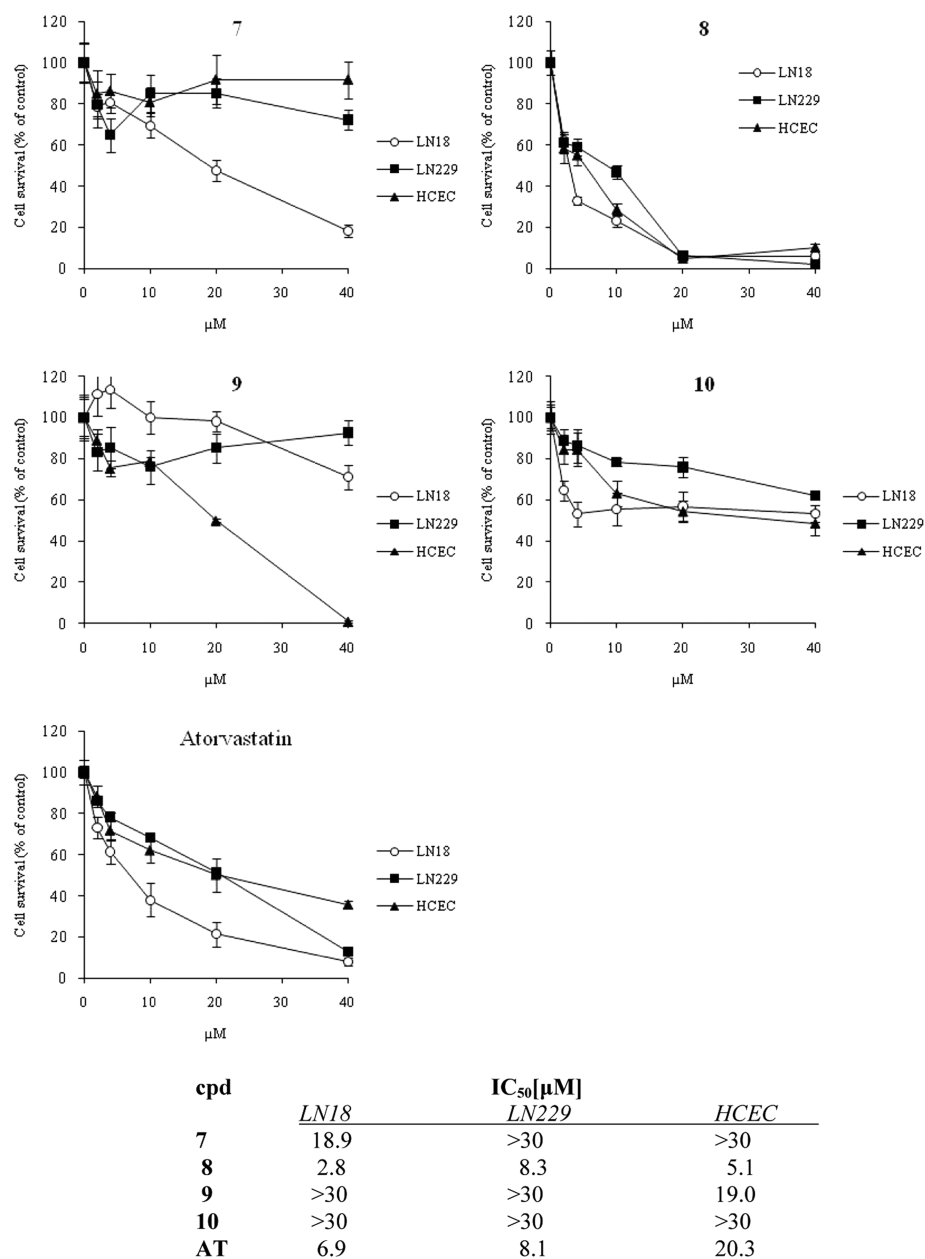


Figure 2. Cytotoxic effects of a 72 h exposure of human glioblastoma and brain-derived endothelial cells to OSCi compounds 7–10 and AT. Human LN18, LN229, and HCEC cells were exposed to increasing concentrations of compounds 7–10 and AT for 72 h. Then the MTT assay was performed and IC₅₀ values were calculated. Results are the mean \pm sd of triplicates of two independent experiments. IC₅₀ values are the mean (sd not shown, $\leq 10\%$ of the values of the means) of triplicates of two independent experiments.

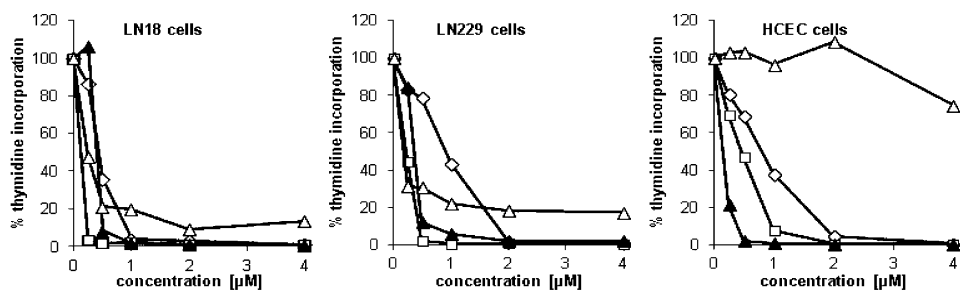


Figure 3. DNA synthesis in glioblastoma and endothelial cells exposed to OSCi or AT. Human LN18, LN229, and HCEC cells were exposed for 24 h to increasing concentrations of OSCi compounds 2–4 and AT. Then [³H]T incorporation was performed to evaluate DNA synthesis. Results are the mean of triplicates (sd not shown, $< 10\%$ of the values of the means): \diamond , 2; \square , 3; \blacktriangle , 4; \triangle , AT.

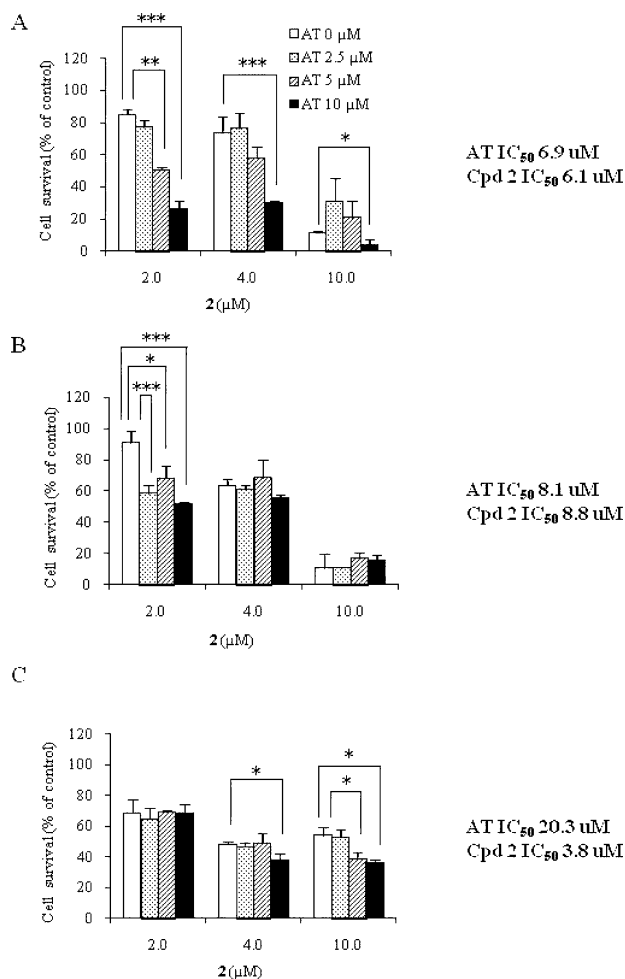


Figure 4. Cytotoxic effects of a 72 h cell exposure to 2-AT combination. Human LN18 (A), LN229 (B), and HCEC (C) cells were treated with 2, 4, and 10 μM OSCi 2 in combination with 2.5, 5, and 10 μM AT for 72 h. Then the MTT assay was performed. Results are the mean \pm sd of triplicates of two independent experiments. Treated cells were compared to untreated cells using the Student's *t*-test: *, $p < 0.05$; **, $p < 0.01$; ***, $p < 0.001$.

synergistic, self-limited, negative regulatory loop to deplete cancer cells from cholesterol. In support of this hypothesis additive effects of OSCi in combination with AT were demonstrated in human glioblastoma cells while maintaining selectivity against endothelial cells. Our results also suggest that the lipophilicity of the OSCi must be taken into account for selectivity, meaning that a more polar OSCi is more selective for inhibiting the growth of cancer cells and for further development of anti-cholesterol compounds in the context of cancer therapy. In summary, we have shown that not only statins targeting HMG-CoA reductase but also inhibitors of OSC decrease tumor cell growth, suggesting new therapeutic opportunities of combined anti-cholesterol agents for dual treatment of glioblastoma.

EXPERIMENTAL SECTION

Chemistry. General. The syntheses and characterizations of compounds 1–4, 8, and 9^{17–20,29} have been previously described. The detailed synthesis and characterization of intermediate compounds 12–16 and 18–23 are provided as Supporting Information.

Reactions were carried out under an atmosphere of argon. Solvents and reagents were obtained from commercial sources and were used as

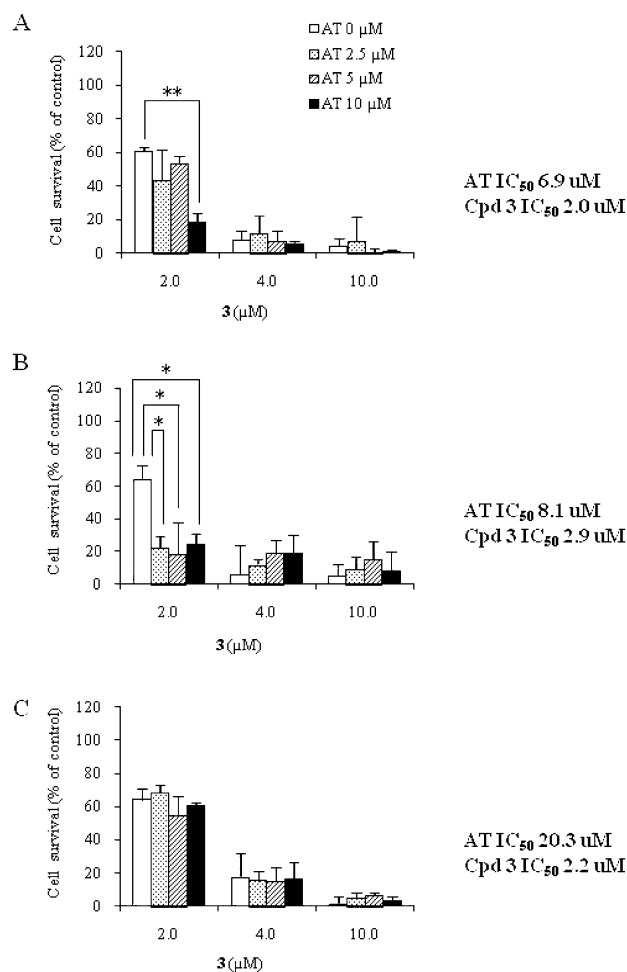


Figure 5. Cytotoxic effects of a 72 h cell exposure to 3-AT combination. Human LN18 (A), LN229 (B), and HCEC (C) cells were treated with 2, 4, and 10 μM OSCi 3 in combination with 2.5, 5, and 10 μM AT for 72 h. Then the MTT assay was performed. Results are the mean \pm sd of triplicates of two independent experiments. Treated cells were compared to untreated cells using the Student's *t*-test: *, $p < 0.05$; **, $p < 0.01$.

received. All reactions were followed by TLC (TLC plates F254, Merck). Proton and carbon NMR spectra were obtained on a Bruker 300, 400, or 600 MHz instrument. The respective carbon NMR spectra were 75, 100, and 150 MHz. The chemical shifts (δ in ppm) are reported relative to tetramethylsilane as internal standard. NMR abbreviations are as follows: s, singlet; d, doublet; t, triplet; q, quadruplet; quint, quintuplet; m, multiplet; br, broadened. Purity was analyzed by ¹H NMR. In the ¹H NMR spectra, the acidic protons of the fumarate, HCl, and citrate salts were not seen unless listed. Mass spectra were recorded on an SSQ7000 (Finnigan-MAT) spectrometer for electron impact ionization. LC-MS (liquid chromatography-mass spectrometry) data were recorded on an Agilent 1290 LC with CTC PAL coupled to Agilent 6520 QTOF. HPLC was performed on Zorbax Eclipse Plus C18 2.1 mm \times 50 mm, 1.8 μm (Agilent catalog no. 959757-902). Column temperature was 55°C. A gradient from 5% to 99% of eluent B in eluent A was used at a flow rate of 1 mL/min. Eluent B consisted of 80% acetonitrile/20% isopropanol/0.01% formic acid. Eluent A was 0.02% formic acid in water. UV detector was DAD, 220 \pm 5 nm or 265 \pm 35 nm. All compounds were characterized by ¹H NMR and MS and final compounds with microanalyses. Elemental analyses were performed by Solvias AG (Mattenstrasse, Postfach, CH-4002 Basel, Switzerland). Results of elemental analyses were within 0.4% of theoretical values. Solvents (¹H NMR) and H₂O content (Karl Fischer determination) were incorporated in the formula. Melting

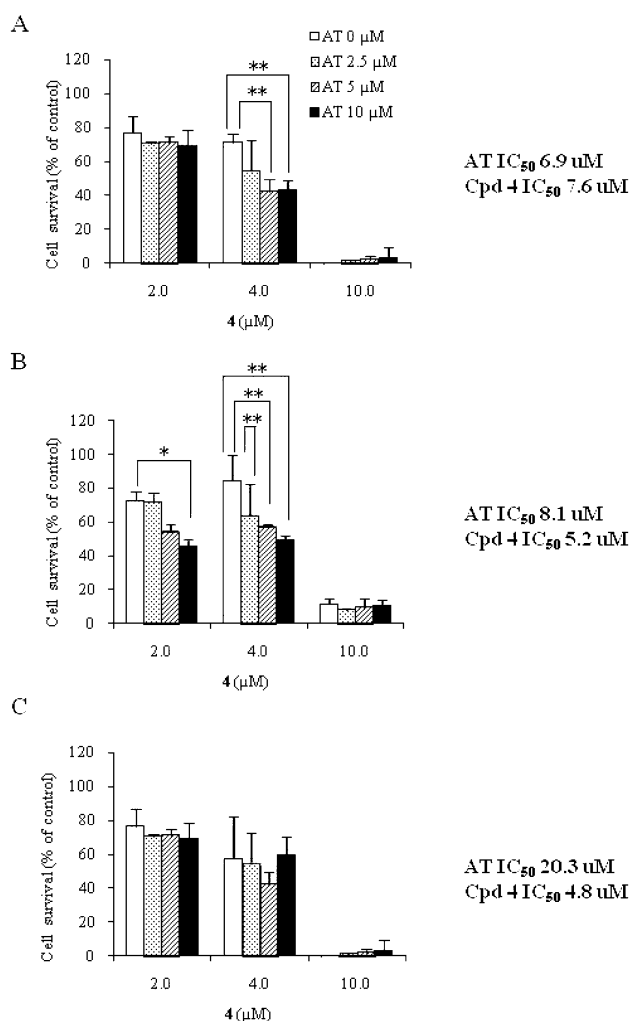


Figure 6. Cytotoxic effects of a 72 h cell exposure to 4-AT combination. Human LN18 (A), LN229 (B), and HCEC (C) cells were treated with 2, 4, and 10 μM OSCi 4 in combination with 2.5, 5, and 10 μM AT for 72 h. Then the MTT assay was performed. Results are the mean \pm sd of triplicates of two independent experiments. Treated cells were compared to untreated cells using the Student's *t*-test: *, $p < 0.05$; **, $p < 0.01$; ***, $p < 0.001$.

points (uncorrected) were determined using a Büchi 510 apparatus and are uncorrected. Silica gel 60 (0.04–0.063 mm, Merck) was used for flash chromatography. The purities of final compounds **5**, **6**, **7**, and **10** were analyzed by LC-MS and by elemental analysis and were found to be above 95%.

trans-[4-[5-[ethyl-(2-hydroxyethyl)amino]pent-1-ynyl]cyclohexyl]methylcarbamic Acid 4-Chlorophenyl Ester Hydrochloride (**5**). A solution of *trans*-methanesulfonic acid 5-(4-methylaminocyclohexyl)pent-4-ynyl ester trifluoroacetate (**16**) (0.57 g, 1.33 mmol) and ethyl-(2-hydroxyethyl)amine (1.29 mL, 13.27 mmol, 10 equiv) in MeOH (13 mL) was stirred overnight at 65 °C. The appropriate portion was extracted with aqueous saturated NaHCO₃ solution/Et₂O (3 \times) and aqueous 10% NaCl solution, and the organic phases were dried over Na₂SO₄, filtered, and evaporated. Purification by flash column chromatography on silica gel (CH₂Cl₂, then CH₂Cl₂/MeOH, 95:5 to 9:1) gave *trans*-[4-[5-[ethyl-(2-hydroxyethyl)amino]pent-1-ynyl]cyclohexyl]methylcarbamic acid 4-chlorophenyl ester (0.35 g, 63%). MS *m/z*: 421.4 (M + H⁺, 1Cl). The amine was dissolved in dioxane (1 mL) and treated with 4 M HCl in dioxane (0.17 mL, 0.69 mmol, 1.1 equiv), filtered, and evaporated. Dissolving in CH₂Cl₂ and evaporation (3 \times) gave after drying in high vacuum the desired compound as a yellow viscous oil (0.36 g, 59% over two steps).

¹H NMR (400 MHz, DMSO-*d*₆, rt) δ 9.36 (broad s, 1H), 7.43 and 7.15 (AA'-BB'-system, J_{AB} = 8.8 Hz, 4H), 5.32 (broad s, 1H), 3.9 and 3.8 (broad m, 1H, 3:1 mixture of rotamers), 3.70 (broad s, 2H), 3.2–3.0 (broad s, 6H), 2.88 and 2.79 (broad s, 3H, 3:1 mixture of rotamers), 2.23 (m, 3H), 1.95 (m, 2H), 1.85–1.55 (m, 6H), 1.39 (m, 2H), 1.18 (m, 3H). ¹³C NMR (400 MHz, DMSO-*d*₆, 120 °C) δ 7.33–7.40 (m, 2H), 7.08–7.16 (m, 2H), 3.79–3.90 (m, 1H), 3.76 (t, J = 5.4 Hz, 2H), 3.06–3.22 (m, 6H), 2.86 (s, 3H), 2.25 (td, J = 6.9, 2.0 Hz, 2H), 2.15–2.22 (m, 1H), 1.93–2.04 (m, 2H), 1.77–1.88 (m, 2H), 1.68–1.75 (m, 2H), 1.60 (qd, J = 12.5, 3.4 Hz, 2H), 1.34–1.47 (m, 2H), 1.25 (t, J = 7.2 Hz, 3H). ¹⁵C NMR (151 MHz, DMSO-*d*₆) δ 156.6, 153.2, 150.1, 129.1, 123.7, 85.0, 78.4, 55.2, 53.8, 50.6, 47.6, 40.0, 32.2, 28.8, 28.2, 28.0, 22.3, 15.4. MS *m/z*: 421.2 (M + H⁺, 1Cl). Anal. (C₂₃H₃₃ClN₂O₃·1.08HCl·1.6H₂O) C, H, N, Cl.

trans-Methyl-[4-[5-(methylpropylamino)pent-1-ynyl]cyclohexyl]carbamic acid 4-Chloro-Phenyl Ester Fumarate (**6**). A solution of *trans*-methanesulfonic acid 5-(4-methylaminocyclohexyl)pent-4-ynyl ester trifluoroacetate (**16**) (0.84 mg, 1.96 mmol) and *N*-methylpropylamine (3.02 mL, 29.44 mmol, 15 equiv) in MeOH (15 mL) was treated with sodium iodide (0.03 g, 0.2 mmol, 0.1 equiv), and the mixture was stirred overnight at 60 °C. The appropriate portion was extracted with aqueous saturated NaHCO₃ solution/Et₂O (3 \times) and aqueous 10% NaCl solution, and the organic phases were dried over Na₂SO₄, filtered, and evaporated. Purification by flash column chromatography on silica gel (CH₂Cl₂, then CH₂Cl₂/MeOH, 95:5 to 9:1) gave *trans*-methyl-[4-[5-(methylpropylamino)pent-1-ynyl]cyclohexyl]carbamic acid 4-chlorophenyl ester (0.75 g, 94%). MS *m/z*: 405.5 (M + H⁺, 1Cl).

The amine (0.7 g, 1.73 mmol) in EtOAc and fumaric acid (0.21 g, 1.81 mmol, 1.05 equiv) in EtOH were mixed and evaporated with EtOAc (3 \times). Slow (24 h) cooling of an EtOAc solution to 4 °C gave crystals. Filtration and washing with a small amount of EtOAc gave the desired product as white crystals (0.73 g, 81%). Mp: 95–98 °C (dec). ¹H NMR (300 MHz, DMSO-*d*₆) δ 7.43 and 7.15 (AA'-BB'-system, J_{AB} = 8.8 Hz, 4H), 6.55 (s, 2H), 3.82 (broad s, 1H), 2.88 and 2.78 (s, 3H, 3:1 mixture of rotamers), 2.55–2.4 (broad m, 4H), 2.29 (s, 3H), 2.16 (t, J = 6.8 Hz, 3H), 1.92 (m, 2H), 1.75–1.25 (m, 10H), 0.85 (t, J = 7.3 Hz, 3H). ¹³C NMR (300 MHz, DMSO-*d*₆ + D₂O) δ 7.43 and 7.15 (AA'-BB'-system, J_{AB} = 8.8 Hz, 4H), 6.49 (s, 2), 3.80 (broad s, 1H), 2.95–2.70 (m, 7H), 2.57 (s, 3H), 2.20 (t, J = 6.0 Hz, 3H), 1.95 (m, 2H), 1.80–1.50 (m, 8H), 1.50–1.30 (m, 2H), 0.89 (t, J = 7.4 Hz, 3H). ¹⁵C NMR (101 MHz, DMSO-*d*₆, 120 °C) δ 165.9, 153.3, 150.5, 133.8, 129.1, 128.9, 123.2, 84.0, 79.9, 59.1, 55.8, 55.2, 41.7, 32.6, 29.1, 28.8, 28.4, 26.4, 19.8, 16.0, 11.4. MS *m/z*: 405.5 (M + H⁺, 1Cl). Anal. (C₂₃H₃₃ClN₂O₂·C₄H₄O₄·0.15H₂O) C, H, N, Cl.

trans-[2-(4-[ethyl-(2-hydroxyethyl)amino]methyl]cyclohexyl)ethyl]methylcarbamic Acid 4-Trifluoromethylphenyl Ester Citrate (**7**). A solution of *trans*-methanesulfonic acid 4-[2-[methyl-(4-trifluoromethylphenoxy)carbonyl]amino]ethyl]cyclohexylmethyl ester (**21**) (0.58, 1.33 mmol) and ethyl-(2-hydroxyethyl)amine (1.29 mL, 13.26 mmol, 10 equiv) in DMA (6 mL) was stirred for 3 days at 60 °C. The appropriate portion was extracted with aqueous 0.25 M NaOH/Et₂O (3 \times), water, and aqueous saturated NaCl solution, and the organic phases were dried over MgSO₄, filtered, and evaporated. Purification by flash column chromatography on silica gel (CH₂Cl₂/MeOH, 95:5) gave *trans*-[2-(4-[ethyl-(2-hydroxyethyl)amino]methyl]cyclohexyl)ethyl]methylcarbamic acid 4-trifluoromethylphenyl ester (0.38 g, 67%). MS *m/z*: 431.3 (M + H⁺).

The amine (2.8 g, 6.50 mmol) and citric acid monohydrate (1.37 g, 6.50 mmol) were dissolved in hot EtOAc (28 mL)/*i*-PrOH (1.6 mL), then slowly (48 h) cooled to –20 °C. After 24 h additional *n*-pentane (10 mL) was mixed in to give after filtration and washing with a small amount of *n*-pentane the desired product as white crystals (3.76 g, 93%). Mp: 64 °C (slow dec). ¹H NMR (400 MHz, DMSO-*d*₆, 120 °C) δ 8.08–10.06 (br s, <3H) 7.61–7.78 (m, 2H), 7.23–7.39 (m, 2H), 3.57 (t, J = 6.0 Hz, 2H), 3.38 (dd, J = 8.1, 7.3 Hz, 2H), 2.75–2.86 (m, 4H), 2.59 (d, J_{AB} = 15.3 Hz, 2H), 2.68 (d, J_{AB} = 15.3 Hz, 2H), 2.55 (d, J = 6.7 Hz, 2H), 2.60 (br s, 3H), 1.72–1.86 (m, 4H), 1.42–1.59 (m, 3H), 1.19–1.33 (m, 1H), 1.07 (t, J = 7.1 Hz, 3H), 0.82–1.04 (m, 4H). ¹³C NMR (101 MHz, DMSO-*d*₆, 120 °C) δ ppm 170.8,

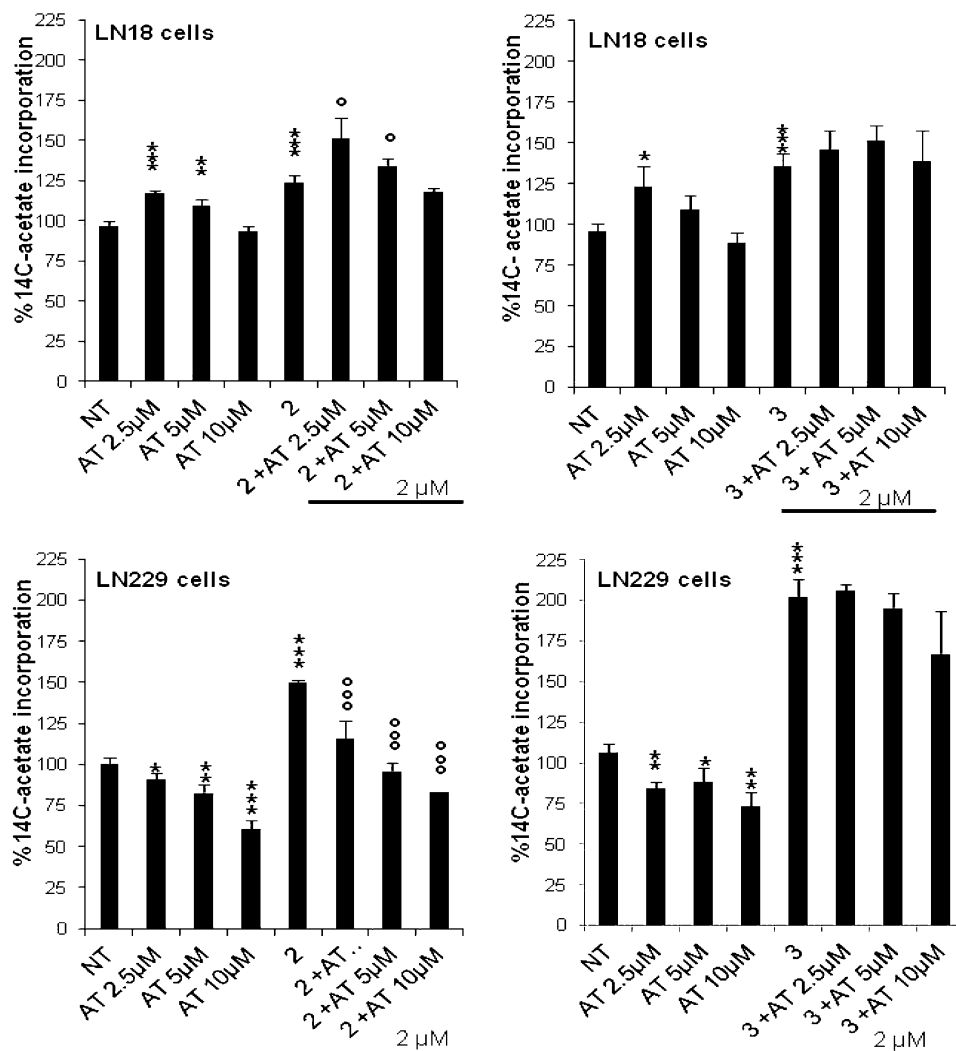


Figure 7. High molecular weight and acid-insoluble lipid synthesis in glioblastoma cells exposed to OSCi and AT. Human LN18 or LN229 cells were exposed for 24 h to increasing concentrations of AT or to 2 μM OSCi 2 or 3 in combination with increasing concentration of AT. Then ¹⁴C-acetate incorporation was performed to evaluate high molecular weight lipid synthesis. Results are the mean of triplicates. Treatments were compared using the Student's *t*-test: *, treated cells vs untreated cells; O, AT–OSCi combination vs OSCi alone; * and O, *p* < 0.05; ** and OO, *p* < 0.01; *** and OOO, *p* < 0.001.

154.6, 153.1, 126.4 (*q*, *J* = 3.8), 122.1, 72.0, 60.6, 57.9, 56.1, 49.0, 47.0, 43.7, 35.2, 35.0, 34.6, 32.2, 30.9, 10.4. MS *m/z*: 431.3 (*M* + *H*⁺). Anal. (C₂₂H₃₃F₃N₂O₃·C₆H₈O₇·0.06H₂O) C, H, N, F.

trans-{2-[4-(4-Hydroxypiperidine-1-carbonyl)cyclohexyl]ethyl}-methylcarbamic Acid 4-Chlorophenyl Ester (**10**). A mixture of *trans*-4-(2-methylaminoethyl)cyclohexanecarboxylic acid·HCl (**23**) (9.75 g, 43.9 mmol) in hexamethyldisilazane (115 mL, 552 mmol, 12 equiv) was heated under reflux to 145 °C for 2.5 h. The solution was evaporated. The residue was suspended in THF (200 mL) and treated with 4-chlorophenyl chloroformate (6.77, 48.4 mmol, 1.1 equiv) at 0 °C, and the mixture was stirred at room temperature overnight. Water (10 mL) was added at room temperature followed by aqueous 1 M NaOH (110 mL, 2.5 equiv). Stirring was continued for 1 h at room temperature. The organic solvent was evaporated and the residue partitioned between *n*-hexane (3×) and H₂O. The water phase was acidified with 1 M HCl and extracted with EtOAc (3×). This organic phase was dried over Na₂SO₄, filtered, and evaporated to yield the crude product. This residue was again partitioned between Et₂O (3×) and aqueous saturated NaHCO₃ solution. The aqueous phase was acidified with aqueous 1 N HCl and extracted with EtOAc (3×). Drying over Na₂SO₄ and evaporation gave pure *trans*-4-[2-[(4-chlorophenoxy-carbonyl)methylamino]ethyl]cyclohexanecarboxylic acid as a brown oil (8.56 g, 57%). MS *m/z*: 338.1 (*M* – *H*⁺, 1Cl).

A solution of *trans*-4-[2-[(4-chlorophenoxy-carbonyl)methylamino]ethyl]cyclohexanecarboxylic acid (7.46 g, 21.95 mmol) in CH₂Cl₂ (200 mL) was treated at room temperature with 2 drops of DMF, followed by oxalyl chloride (0.28 mL, 2.08 mmol, 1.1 equiv) within 5 min, and stirring was continued for 90 min. The solution was evaporated, redissolved in CH₂Cl₂ (200 mL), and added to a cooled solution (0 °C) of 4-hydroxypiperidine (6.66 g, 65.86 mmol, 3 equiv) and Et₃N (15.30 mL, 109.76 mmol, 5 equiv) in CH₂Cl₂ (120 mL). The mixture was kept at room temperature for 1.5 h and then partitioned between Et₂O (3×) and aqueous 10% KHSO₄ solution. The organic phases were washed once with aqueous 10% NaCl solution, dried over Na₂SO₄, filtered, and evaporated to give the desired product (9.00 g, 97%). ¹H NMR (300 MHz, DMSO-*d*₆) δ 7.43 and 7.13 (AA'-BB'-system, two rotamers, 4H), 4.71 (d, *J* = 10.5 Hz, 1H), 3.82 (m, 1H), 3.66 (m, 2H), 3.39 (m, 1H), 3.30 (m, 1H), 3.15 (m, 1H), 3.00 and 2.88 (s, 3H, 4:5 mixture of rotamers), 2.94 (m, 1H), 1.84–1.58 (m, 6H), 1.56–0.90 (m, 10H). ¹H NMR (400 MHz, DMSO-*d*₆, 120 °C) δ 7.30–7.45 (m, 2H), 7.03–7.17 (m, 2H), 4.21 (d, *J* = 4.3 Hz, 1H), 3.74–3.83 (m, 2H), 3.66–3.74 (m, 1H), 3.31–3.40 (m, 2H), 3.03–3.14 (m, 2H), 2.95 (s, 3H), 2.49–2.54 (m, 1H), 1.75–1.84 (m, 2H), 1.61–1.75 (m, 4H), 1.45–1.55 (m, 2H), 1.22–1.45 (m, 5H), 0.98–1.11 (m, 2H). ¹³C NMR (101 MHz, DMSO-*d*₆, 120 °C) δ 173.4, 153.5, 150.5, 129.1, 123.2, 65.7, 46.8, 34.7, 34.5, 34.2, 31.9, 29.1.

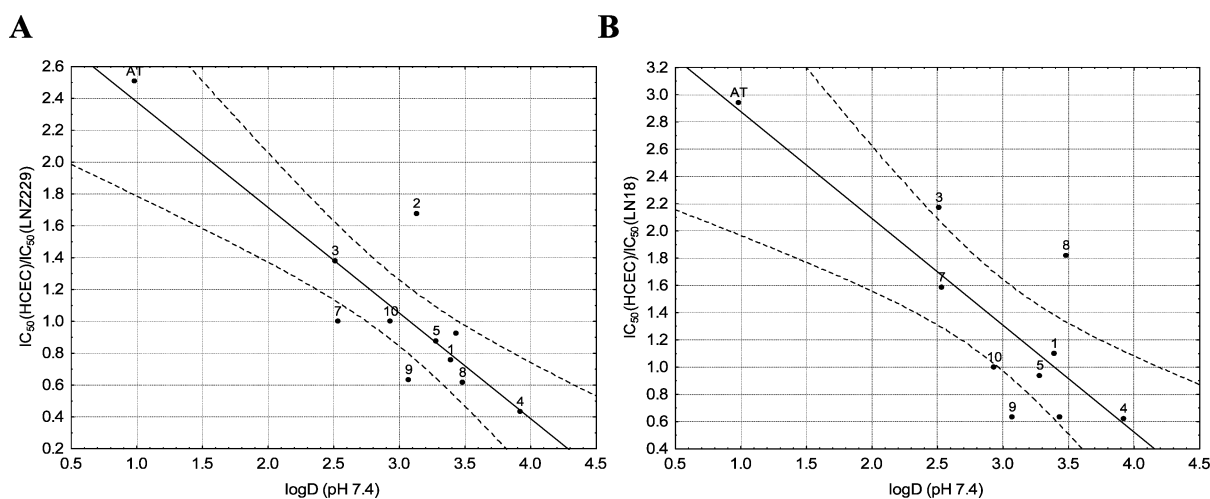


Figure 8. Correlation between $\log D$ and IC_{50} . (A) Correlation of the selectivity ratio $IC_{50}(\text{HCEC})/IC_{50}(\text{LN229})$ with $\log D$ at pH 7.4. Black line represents the regression line ($r^2 = 0.91$; $IC_{50}(\text{HCEC})/IC_{50}(\text{LN229}) = (4.23 \pm 0.17) - (\log D)(1.33 \pm 0.15)$), and dotted lines represent the 95% confidence interval. Cross-validation coefficient (leave-one-out method) is $q^2 = 0.88$. (B) Correlation of the selectivity ratio $IC_{50}(\text{HCEC})/IC_{50}(\text{LN18})$ with $\log D$ at pH 7.4. Black line represents the regression line ($r^2 = 0.69$; $IC_{50}(\text{HCEC})/IC_{50}(\text{LN229}) = (4.13 \pm 0.32) - (\log D)(0.87 \pm 0.21)$), and dotted lines represent the 95% confidence interval. Cross-validation coefficient (leave-one-out method) is $q^2 = 0.66$.

MS m/z : 423.2 ($M + H^+$, 1Cl). Anal. ($C_{22}H_{31}ClN_2O_4 \cdot 0.55H_2O \cdot 0.12C_2H_6O$) C, H, N, Cl.

Physicochemical Characterization of the Inhibitors. $\log D$ Determination. The high-throughput assay method is derived from the conventional "shake flask" method. The compound of interest is distributed between a 50 mM aqueous 3-[[1,3-dihydroxy-2-(hydroxymethyl)propan-2-yl]amino]-2-hydroxypropane-1-sulfonic acid (TAPSO) buffer at pH 7.4 and 1-octanol. The distribution coefficient is then calculated from the difference in concentration in the aqueous phase before and after partitioning and the volume ratio of the two phases. A detailed description of the method can be found elsewhere.³⁸

PAMPA. For PAMPA, a "sandwich" is formed from a 96-well filter plate and a 96-well in-house-made Teflon plate such that each well is divided into two chambers: donor at the bottom and acceptor at the top, separated by a microfilter coated with a 10% (w/v) egg-phosphatidylcholine and 0.5% (w/v) cholesterol dissolved in dodecane. The distribution of a compound between the top compartment, the artificial membrane, and the bottom compartment is then determined. A detailed description of the method can be found elsewhere.³⁹

Biology. Evaluation of OSC Inhibition. Inhibition of human liver microsomal 2,3-OSC was used to evaluate the inhibitory potency of the new molecules, essentially as described previously.¹⁹ Briefly, OSC activity was measured in human liver microsomes in sodium phosphate buffer–EDTA–dithiothreitol, pH 7.4. The inhibitors were dissolved in DMSO and diluted to the desired concentration in the buffer. [¹⁴C] R,S-MOS (12.8 mCi/mmol, 1 mM final concentration, 20 nCi/ μ l) in phosphate buffer/1% BSA was mixed with the microsomes, and the reaction proceeded for 1 h at 37 °C. The reaction was stopped by the addition of 10% KOH/MeOH. Then *n*-hexane/Et₂O containing non-radioactive MOS and lanosterol as carriers was added. After shaking, the upper phase was evaporated and suspended in *n*-hexane/Et₂O and applied to a silica gel plate for chromatographic separation using *n*-hexane/Et₂O as the eluent. Radioactive MOS and lanosterol were detected on the silica gel plate using a phosphor imager (Molecular Dynamics). The ratio of MOS to lanosterol was determined from the radioactive bands in order to determine the yield of the reaction and OSC inhibition.

Cells and Cell Treatments. Human A549 lung, CaCo2 colon, HeLa cervix, LnCap prostate, MCF-7 breast, OVCAR ovarian, and LN229 glioblastoma cancer cells are available from the ATCC (American Tissue Culture Collection, Manassas, VA, U.S.). Human LN18 and LN2308 glioblastoma cells were a kind gift from AC Diserens, CHUV, Lausanne, Switzerland. Human Me300 melanoma cells were from D. Rimoldi, Ludwig Institute, Lausanne branch, Switzerland, and KB head

and neck cancer cells were from M. Barberi Heyob, University of Nancy, France. The human-brain-derived HCEC microvascular endothelial cell line was a kind gift of D. Staminovic (Ottawa, Canada). All cells were grown in Dulbecco's modified Eagle medium (DMEM) medium containing 4.5 g/L glucose, 10% heat-inactivated fetal calf serum (FCS), and penicillin/streptomycin (all cell culture reagents were obtained from Invitrogen, Basel, Switzerland). Unless otherwise specified, cells were grown for 24 h in 48-well plates (Costar, Corning, NY, U.S.). Then the compounds were added for the indicated times and concentrations. Compounds 2, 3, 5, 6, 7, 8, and 9 were dissolved at 50 mM in water and compounds 1, 4, 10, and AT in DMSO, and then they were diluted to 1 mM in cell culture medium containing FCS immediately before use.

Determination of Cytotoxicity. Following exposure to the compounds, cell viability was assessed using the MTT assay (3-(4,5-dimethyl-2-thiazoyl)-2,5-diphenyltetrazolium bromide, Sigma-Aldrich, 200 μ g/mL final concentration), essentially as previously described.⁵² Absorbance at 540 nm was measured in a multiwell plate reader (iEMS Reader, Labsystems, Bioconcept, Allschwil, Switzerland), and the absorbance values of treated cells were compared to the absorbance values of untreated cells. Experiments were conducted in triplicate wells and repeated twice. The mean \pm standard deviation (sd) values were calculated.

Evaluation of DNA Synthesis. Following cell exposure to the compounds for 48 h, tritiated thymidine ([³H]T) (Amersham-Pharmacia, Glattbrugg, Switzerland, 400 nCi/mL final concentration) was added to the cells for 2–4 h. Then the cell layers were precipitated with 10% TCA and dissolved in 0.1% sodium dodecyl sulfate (SDS) in 0.1 N NaOH, and scintillation cocktail (Optiphase HI-Safe, PerkinElmer, Beaconsfield, U.K.) was added. Radioactivity was counted with a β -counter (WinSpectra, Wallac, Germany). The radioactivity counts of treated cells were compared to the radioactivity counts of untreated cells. Experiments were conducted in triplicate wells, and the mean \pm sd values were calculated.

Acetate Incorporation. Cells were seeded in a 48-well plate for 24 h and exposed to the chemicals for 24 h. Then [¹⁴C]sodium acetate (American Radiolabeled Chemicals, St. Louis, MO, U.S.; 10 nCi/mL final concentration) was added to the cells for 7.5 h. The cell layers were precipitated with 10% TCA and dissolved in 0.1% SDS in 0.1 N NaOH and scintillation cocktail (Optiphase HI-Safe). Radioactivity was counted in a β -counter (WinSpectra). The radioactivity counts of treated cells were compared to the radioactivity counts of untreated cells. Experiments were conducted in triplicate wells, and the mean \pm sd values were calculated.

Evaluation of Results. Each experiment was repeated in triplicate wells at least twice. The mean and standard deviation values were calculated, and statistical significance was evaluated using the Student's *t*-test.

Squared cross-validation coefficients according to the leave-one-out method (q^2) and the squared correlation coefficients (r^2) were calculated with SIMCA, version 12 (Umetrics Inc., Umea, Sweden).

■ ASSOCIATED CONTENT

■ Supporting Information

Detailed protocols for chemical synthesis and characterization of compounds 12–16 and 18–23; in vitro inhibitory stability and chemical stability of OSCi 1–10; cytotoxicity of compounds 1–10 and AT after 24–72 h of cell exposure; IC₅₀ values for inhibition of DNA synthesis after 24 h of exposure of cells to compounds 1–10 and AT; evaluation of synergism or additivity of the effects of combination of compounds with AT in human endothelial and glioblastoma cells; evaluation of synergism of the effects of combination of compound 3 with AT in human LN229 glioblastoma cells. This material is available free of charge via the Internet at <http://pubs.acs.org>.

■ AUTHOR INFORMATION

Corresponding Author

*For L.J.-J.: phone, +41 21 314 7173; fax, +41 21 314 7115; e-mail, lucienne.juillerat@chuv.ch. For J.D.A.: phone, +41 61 688 7738; fax, +41 61 688 8367; e-mail, johannes.aebi@roche.com.

Notes

The authors declare no competing financial interest.

■ ACKNOWLEDGMENTS

We sincerely thank Dr. Jean Ackermann, Dr. Christian Jenny, Dr. Francois Montavon, Felix Gruber, Marie-Paule Imhoff, Isabelle Kaufmann, Fritz Koch, Hans-Jakob Krebs, and Anke Kurt for their excellent and dedicated assistance; Dr. Olivier Morand, Gisela Flach, Corinne Handschin, and Elisabeth Von Der Mark for the OSC inhibition data; Dr. Caroline Wyss Gramberg, Dr. Inken Plitzko, Dr. Josef Schneider, and Christian Bartelmus for spectroscopic determination and analysis; Isabelle Parilla, Bjoern Wagner, and Severin Wendelspiess for determining the MDO data.

■ ABBREVIATIONS USED

AT, atorvastatin; Boc, *tert*-butyloxycarbonyl; BSA, bovine serum albumin; BuLi, butyllithium; CI, combination index; CNS, central nervous system; DMEM, Dulbecco's modified Eagle Mmedium; EDCl, *N*-(3-dimethylaminopropyl)-*N*'-ethylcarbodiimide hydrochloride; FCS, fetal calf serum; HCEC, human cerebral endothelial cell; HMG-CoA, 3-hydroxy-3-methylglutaryl coenzyme A; HOBT, 1-hydroxybenzotriazole hydrate; [³H]T, tritiated thymidine; IC₅₀, concentration inhibiting 50% of enzymatic activity; II, interaction index; LN18, LN229, human glioblastoma cells; MOS, monooxidosqualene; MTT, 3-(4,5-dimethyl-2-thiazoyl)-2,5-diphenyltetrazolium bromide; OSC, oxidosqualene cyclase; OSCi, oxidosqualene cyclase inhibitor; PAMPA, parallel artificial membrane permeation assay; P_e , permeability; *i*-Pr₂NEt, *N*-ethyl-diisopropylamine; SDS, sodium dodecyl sulfate; TAPSO, 3-[[1,3-dihydroxy-2-(hydroxymethyl)propan-2-yl]amino]-2-hydroxypropane-1-sulfonic acid; TCA, trichloroacetic acid

■ REFERENCES

- (1) Maxfield, F. R.; Tabas, I. Role of cholesterol and lipid organization in disease. *Nature* **2005**, *438*, 612–621.
- (2) Raposo, G.; Stenmark, H. Membranes and organelles. *Curr. Opin. Cell Biol.* **2008**, *20*, 357–359.
- (3) Nissen, S. E.; Tuzcu, E. M.; Schoenhagen, P.; Crowe, T.; Sasiela, W. J.; Tsai, J.; Orazem, J.; Magorien, R. D.; O'Shaughnessy, C.; Ganz, P. Statin therapy, LDL cholesterol, C-reactive protein, and coronary artery disease. *N. Engl. J. Med.* **2005**, *352*, 29–38.
- (4) Mills, E. J.; Rachlis, B.; Wu, P.; Devereaux, P. J.; Arora, P.; Perri, D. Primary prevention of cardiovascular mortality and events with statin treatments: a network meta-analysis involving more than 65,000 patients. *J. Am. Coll. Cardiol.* **2008**, *52*, 1769–1781.
- (5) Demierre, M. F.; Higgins, P. D.; Gruber, S. B.; Hawk, E.; Lippman, S. M. Statins and cancer prevention. *Nat. Rev. Cancer* **2005**, *5*, 930–942.
- (6) Chan, K. K.; Oza, A. M.; Siu, L. L. The statins as anticancer agents. *Clin. Cancer Res.* **2003**, *9*, 10–19.
- (7) Cemeus, C.; Zhao, T. T.; Barrett, G. M.; Lorimer, I. A.; Dimitroulakos, J. Lovastatin enhances gefitinib activity in glioblastoma cells irrespective of EGFRvIII and PTEN status. *J. Neuro-Oncol.* **2008**, *90*, 9–17.
- (8) Guo, D.; Prins, R. M.; Dang, J.; Kuga, D.; Iwanami, A.; Soto, H.; Lin, K. Y.; Huang, T. T.; Akhavan, D.; Hock, M. B.; Zhu, S.; Kofman, A. A.; Bensinger, S. J.; Yong, W. H.; Vinters, H. V.; Horvath, S.; Watson, A. D.; Kuhn, J. G.; Robins, H. I.; Mehta, M. P.; Wen, P. Y.; DeAngelis, L. M.; Prados, M. D.; Mellinghoff, I. K.; Cloughesy, T. F.; Mischel, P. S. EGFR signaling through an Akt-SREBP-1-dependent, rapamycin-resistant pathway sensitizes glioblastomas to antilipogenic therapy. *Sci. Signaling* **2009**, *2*, ra82.
- (9) van de Donk, N. W.; Kamphuis, M. M.; Lokhorst, H. M.; Bloem, A. C. The cholesterol lowering drug lovastatin induces cell death in myeloma plasma cells. *Leukemia* **2002**, *16*, 1362–1371.
- (10) Graaf, M. R.; Richel, D. J.; van Noorden, C. J.; Guchelaar, H. J. Effects of statins and farnesyltransferase inhibitors on the development and progression of cancer. *Cancer Treat. Rev.* **2004**, *30*, 609–641.
- (11) Vincent, L.; Chen, W.; Hong, L.; Mirshahi, F.; Mishal, Z.; Mirshahi-Khorassani, T.; Vannier, J. P.; Soria, J.; Soria, C. Inhibition of endothelial cell migration by cerivastatin, an HMG-CoA reductase inhibitor: contribution to its anti-angiogenic effect. *FEBS Lett.* **2001**, *495*, 159–166.
- (12) Park, H. J.; Kong, D.; Iruela-Arispe, L.; Begley, U.; Tang, D.; Galper, J. B. 3-Hydroxy-3-methylglutaryl coenzyme A reductase inhibitors interfere with angiogenesis by inhibiting the geranylgeranylation of RhoA. *Circ. Res.* **2002**, *91*, 143–150.
- (13) Weis, M.; Heeschen, C.; Glassford, A. J.; Cooke, J. P. Statins have biphasic effects on angiogenesis. *Circulation* **2002**, *105*, 739–745.
- (14) Dulak, J.; Jozkowicz, A. Anti-angiogenic and anti-inflammatory effects of statins: relevance to anti-cancer therapy. *Curr. Cancer Drug Targets* **2005**, *5*, 579–594.
- (15) Jakobisiak, M.; Golab, J. Statins can modulate effectiveness of antitumor therapeutic modalities. *Med. Res. Rev.* **2010**, *30*, 102–135.
- (16) Perchellet, J. P.; Perchellet, E. M.; Crow, K. R.; Buszek, K. R.; Brown, N.; Ellappan, S.; Gao, G.; Luo, D.; Minatoya, M.; Lushington, G. H. Novel synthetic inhibitors of 3-hydroxy-3-methylglutaryl-coenzyme A (HMG-CoA) reductase activity that inhibit tumor cell proliferation and are structurally unrelated to existing statins. *Int. J. Mol. Med.* **2009**, *24*, 633–643.
- (17) Morand, O. H.; Aebi, J. D.; Dehmlow, H.; Ji, Y. H.; Gains, N.; Lengsfeld, H.; Himber, J. Ro 48-8071, a new 2,3-oxidosqualene:lanosterol cyclase inhibitor lowering plasma cholesterol in hamsters, squirrel monkeys, and minipigs: comparison to simvastatin. *J. Lipid Res.* **1997**, *38*, 373–390.
- (18) Balliano, G.; Dehmlow, H.; Oliaro-Bosso, S.; Scaldaferrri, M.; Taramino, S.; Viola, F.; Caron, G.; Aebi, J.; Ackermann, J. Oxidosqualene cyclase from *Saccharomyces cerevisiae*, *Trypanosoma cruzi*, *Pneumocystis carinii* and *Arabidopsis thaliana* expressed in yeast: a model for the development of novel antiparasitic agents. *Bioorg. Med. Chem. Lett.* **2009**, *19*, 718–723.

- (19) Dehmlow, H.; Aebi, J. D.; Jolidon, S.; Ji, Y. H.; von der Mark, E. M.; Himber, J.; Morand, O. H. Synthesis and structure–activity studies of novel orally active non-terpenoid 2,3-oxidosqualene cyclase inhibitors. *J. Med. Chem.* **2003**, *46*, 3354–3370.
- (20) Lenhart, A.; Reinert, D. J.; Aebi, J. D.; Dehmlow, H.; Morand, O. H.; Schulz, G. E. Binding structures and potencies of oxidosqualene cyclase inhibitors with the homologous squalene–hopene cyclase. *J. Med. Chem.* **2003**, *46*, 2083–2092.
- (21) Rowe, A. H.; Arghmann, C. A.; Edwards, J. Y.; Sawyez, C. G.; Morand, O. H.; Hegele, R. A.; Huff, M. W. Enhanced synthesis of the oxysterol 24(S),25-epoxycholesterol in macrophages by inhibitors of 2,3-oxidosqualene:lanosterol cyclase: a novel mechanism for the attenuation of foam cell formation. *Circ. Res.* **2003**, *93*, 717–725.
- (22) Telford, D. E.; Lipson, S. M.; Barrett, P. H.; Sutherland, B. G.; Edwards, J. Y.; Aebi, J. D.; Dehmlow, H.; Morand, O. H.; Huff, M. W. A novel inhibitor of oxidosqualene:lanosterol cyclase inhibits very low-density lipoprotein apolipoprotein B100 (apoB100) production and enhances low-density lipoprotein apoB100 catabolism through marked reduction in hepatic cholesterol content. *Arterioscler., Thromb., Vasc. Biol.* **2005**, *25*, 2608–2614.
- (23) Gao, J.; Chu, X.; Qiu, Y.; Wu, L.; Qiao, Y.; Wu, J.; Li, D. Discovery of potent inhibitor for farnesyl pyrophosphate synthase in the mevalonate pathway. *Chem. Commun.* **2010**, *46*, 5340–5342.
- (24) Mark, M.; Muller, P.; Maier, R.; Eisele, B. Effects of a novel 2,3-oxidosqualene cyclase inhibitor on the regulation of cholesterol biosynthesis in HepG2 cells. *J. Lipid Res.* **1996**, *37*, 148–158.
- (25) Eisele, B.; Budzinski, R.; Müller, P.; Mark, M. Effects of a novel 2,3-oxidosqualene cyclase inhibitor on cholesterol biosynthesis and lipid metabolism in vivo. *J. Lipid Res.* **1997**, *38*, 564–575.
- (26) Dollis, D.; Schuber, F. Effects of 2,3-oxidosqualene-lanosterol cyclase inhibitor, 2,3:22,23-dioxidosqualene and 24,25-epoxycholesterol on the regulation of cholesterol biosynthesis in human hepatoma cell line Hep-G2. *Biochem. Pharmacol.* **1994**, *48*, 49–57.
- (27) Peffley, D. M.; Gayen, A. K.; Morand, O. H. Down-regulation of 3-hydroxy-3-methylglutaryl coenzyme A reductase mRNA levels and synthesis in syrian hamster C100 cells by the oxidosqualene cyclase inhibitor [4'-(6-allyl-ethyl-amino-hexyloxy)-2'-fluoro-phenyl]-(4-bromophenyl)-methanone (RO0488071): comparison to simvastatin. *Biochem. Pharmacol.* **1998**, *56*, 439–449.
- (28) Gardner, R. G.; Shan, H.; Matsuda, S. P. T.; Hampton, R. Y. An oxysterol-derived positive signal for 3-hydroxy-3-methylglutaryl-CoA reductase degradation in yeast. *J. Biol. Chem.* **2001**, *276*, 8681–8694.
- (29) Dehmlow, H.; Ackermann, J.; Aebi, J.; Blum-Kaelin, D.; Chucholowski, A.; Coassolo, P.; Hartman, P.; Kansy, M.; Maerki, H. P.; Morand, O.; Von der Mark, E.; Panday, N.; Ruf, A.; Thoma, R.; Schulz-Gasch, T. Oxidosqualene cyclase (OSC) inhibitors for the treatment of dyslipidemia. *Chimia* **2005**, *59*, 72–76.
- (30) Jolidon, S.; Polak-Wyss, A.; Hartman, P. G.; Guerry, P. 2,3-Oxidosqualenolanosterol Cyclase: An Attractive Target for Antifungal Drug Design. In *Recent Advances in the Chemistry of Anti-Infective Agents*; Bentley, P. H., Ponsford, R., Eds.; Bookcraft Ltd.: Bath, U.K., 1993; pp 223–233.
- (31) Thoma, R.; Schulz-Gasch, T.; D'Arcy, B.; Benz, J.; Aebi, J.; Dehmlow, H.; Hennig, M.; Stihle, M.; Ruf, A. Insight into steroid scaffold formation from the structure of human oxidosqualene cyclase. *Nature* **2004**, *432*, 118–122.
- (32) Corey, E. J.; Fuchs, P. L. Synthetic method for conversion of formyl groups into ethynyl groups. *Tetrahedron Lett.* **1972**, *36*, 3769–3772.
- (33) Li, P.; Yamamoto, H. Amino acid salt catalyzed intramolecular Robinson annulation. *Chem. Commun.* **2009**, *36*, 5412–5414.
- (34) Carlsen, P. H. J.; Katsuki, T.; Martin, V. S.; Sharpless, K. B. A greatly improved procedure for ruthenium tetroxide catalyzed oxidations of organic compounds. *J. Org. Chem.* **1981**, *46*, 3936–3938.
- (35) Brusselmans, K.; Timmermans, L.; Van de Sande, T.; Van Veldhoven, P. P.; Guan, G.; Schechter, I.; Claessens, F.; Verhoeven, G.; Swinnen, J. V. Squalene synthase, a determinant of Raft-associated cholesterol and modulator of cancer cell proliferation. *J. Biol. Chem.* **2007**, *282*, 18777–18785.
- (36) Chou, T. C. Theoretical basis, experimental design, and computerized simulation of synergism and antagonism in drug combination studies. *Pharm. Rev.* **2006**, *58*, 621–681.
- (37) Lee, J. J.; Kong, M.; Ayers, G. D.; Lotan, R. Interaction index and different methods for determining drug interaction in combination therapy. *J. Biopharm. Stat.* **2007**, *17*, 461–480.
- (38) Wuitschik, G.; Carreira, E. M.; Wagner, B.; Fischer, H.; Parrilla, I.; Schuler, F.; Rogers-Evans, M.; Muller, K. Oxetanes in drug discovery: structural and synthetic insights. *J. Med. Chem.* **2010**, *53*, 3227–3246.
- (39) Kansy, M.; Senner, F.; Gubernator, K. Physicochemical high throughput screening: parallel artificial membrane permeability assay in the description of passive absorption processes. *J. Med. Chem.* **1998**, *41*, 1007–1010.
- (40) Bjorkhem, I.; Meaney, S. Brain cholesterol: long secret life behind a barrier. *Arterioscler., Thromb., Vasc. Biol.* **2004**, *24*, 806–815.
- (41) Dietschy, J. M.; Turley, S. D. Cholesterol metabolism in the central nervous system during early development and in the mature animal. *J. Lipid Res.* **2004**, *45*, 1375–1397.
- (42) Natali, F.; Siculella, L.; Salvati, S.; Gnoni, G. V. Oleic acid is a potent inhibitor of fatty acid and cholesterol synthesis in C6 glioma cells. *J. Lipid Res.* **2007**, *48*, 1966–1975.
- (43) Prasanna, P.; Thibault, A.; Liu, L.; Samid, D. Lipid metabolism as a target for brain cancer therapy: synergistic activity of lovastatin and sodium phenylacetate against human glioma cells. *J. Neurochem.* **1996**, *66*, 710–716.
- (44) Brown, R. C.; Cascio, C.; Papadopoulos, V. Pathways of neurosteroid biosynthesis in cell lines from human brain: regulation of dehydroepiandrosterone formation by oxidative stress and beta-amyloid peptide. *J. Neurochem.* **2000**, *74*, 847–859.
- (45) Bababeygy, S. R.; Polevaya, N. V.; Youssef, S.; Sun, A.; Xiong, A.; Pruggichailers, T.; Veeravagu, A.; Hou, L. C.; Steinman, L.; Tse, V. HMG-CoA reductase inhibition causes increased necrosis and apoptosis in an in vivo mouse glioblastoma multiforme model. *Anticancer Res.* **2009**, *29*, 4901–4908.
- (46) Bouterfa, H. L.; Sattelmeyer, V.; Czub, S.; Vordermark, D.; Roosen, K.; Tonn, J. C. Inhibition of Ras farnesylation by lovastatin leads to downregulation of proliferation and migration in primary cultured human glioblastoma cells. *Anticancer Res.* **2000**, *20*, 2761–2771.
- (47) Chan, D. Y. L.; Chen, G. G.; Poon, W. S.; Liu, P. C. Lovastatin sensitized human glioblastoma cells to TRAIL-induced apoptosis. *J. Neuro-Oncol.* **2008**, *86*, 273–283.
- (48) Jiang, Z.; Zheng, X.; Lytle, R. A.; Higashikubo, R.; Rich, K. M. Lovastatin-induced up-regulation of the BH3-only protein, Bim, and cell death in glioblastoma cells. *J. Neurochem.* **2004**, *89*, 168–178.
- (49) Schmidt, F.; Groscurth, P.; Kermer, M.; Dichgans, J.; Weller, M. Lovastatin and phenylacetate induce apoptosis, but not differentiation in human malignant glioma cells. *Acta Neuropathol.* **2001**, *101*, 217–224.
- (50) Tapia-Perez, J. H.; Kirches, E.; Mawrin, C.; Firsching, R.; Schneider, T. Cytotoxic effect of different statins and thiazolidinediones on malignant glioma cells. *Cancer Chemother. Pharmacol.* **2011**, *67*, 1193–1201.
- (51) Larner, J.; Jane, J.; Laws, E.; Packer, R.; Myers, C.; Shaffrey, M. A phase I–II trial of lovastatin for anaplastic astrocytoma and glioblastoma multiforme. *Am. J. Clin. Oncol.* **1998**, *21*, 579–583.
- (52) Berger, Y.; Dehmlow, H.; Blum-Kaelin, D.; Kitas, E. A.; Löffler, B. M.; Aebi, J. D.; Juillerat-Jeanneret, L. Endothelin-converting-enzyme-1 inhibition and growth of human glioblastoma cells. *J. Med. Chem.* **2005**, *48*, 483–498.